Further Generalization of an Equivalent Plate Representation for Aircraft Structural Analysis

Gary L. Giles*
NASA Langley Research Center, Hampton, Virginia

Recent developments from a continuing effort to provide an equivalent plate representation for aircraft structural analysis are described. Previous work provided an equivalent plate analysis formulation that is capable of modeling aircraft wing structures with a general planform such as cranked wing boxes. However, the modeling is restricted to representing wing boxes having symmetric cross sections. Further developments, which are described in this paper, allow modeling of wing cross sections having asymmetries that can arise from airfoil camber or from thicknesses being different in the upper and lower cover skins. An implementation of thermal loadings, which are described as temperature distributions over the planform of the cover skins, has been included. Spring supports have been added to provide for a more general set of boundary conditions. Numerical results are presented to assess the effect of wing camber on the static and dynamic response of an example wing structure under pressure and thermal loading. These results are compared with results from a finite-element analysis program to indicate how well a cambered wing box can be represented with an equivalent plate formulation.

Nomenclature

a,b,c,e,f,g = planform dimensions (see Fig. 3)
A_i,B_j,C_k = coefficients of polynomial displacement functions for U, V, and W components, respectively
h = wing box depth
K_{ij} = stiffness submatrix for i, j displacement components
P_u,P_v,P_w = load vectors corresponding to U,V,W deformations
Q^k = lamina stiffness matrix for kth layer
S_{ij} = components of lamina compliance matrix [see Eq. (6)]
t = thickness of cover skin layer
T = temperature
$U,V,W,$ = displacement functions in the $x,y,z,$ directions, respectively
x,y = global streamwise and spanwise coordinates, respectively
X_i,Y_i = polynomials in x and y for defining displacement functions
z = distance measured normal to reference surface
zc = location of midcamber surface
$\alpha_x,\alpha_y,\alpha_{xy}$ = thermal coefficients of expansion in x-y coordinates
α_1,α_2 = thermal coefficients of expansion along orthotropic material axes
$\varepsilon_x,\varepsilon_y,\varepsilon_{xy}$ = total strains in x-y coordinates
$\varepsilon'_1,\varepsilon'_2,\varepsilon'_{12}$ = stress-induced strains along orthotropic material axes
$\varepsilon''_1,\varepsilon''_2,\varepsilon''_{12}$ = temperature-induced strains along orthotropic material axes
ξ,η = local nondimensional streamwise and spanwise coordinates, respectively
Ω = function used in surface fitting procedure [see Eq. (15)]
Π = potential energy
$\sigma_x,\sigma_y,\sigma_{xy}$ = stresses in x-y coordinates
θ = orientation of orthotropic material axes (see Fig. 1b)
Φ = parameter to define magnitude of wing camber
$(,)$ = denotes differentiation, e.g., $W_{,x} = dW/dx$; $W_{,xy} = d^2W/dx\,dy$

Introduction

SIMPLIFIED beam or plate models of aircraft wing structures are often used for analysis during early preliminary design.[1] For example, an equivalent plate model of the wing structure is used in the TSO (Aeroelastic Tailoring and Structural Optimization) computer program.[2,3] This program has had widespread use for aeroelastic tailoring of composite wings.[4] However, the structural analysis formulation used in TSO is limited to trapezoidal planforms.

Recently, a new equivalent plate analysis formulation has been developed with the capability to model aircraft composite wing structures with general planform geometry such as cranked wing boxes.[5] This formulation contains only bending terms in the expression of the equivalent plate energy. Therefore, the modeling is restricted to representing wing boxes having cross sections that are symmetric about a midplane. Also, all applied loads, such as aerodynamic pressures, must act normal to this midplane.

The present paper describes a further generalization of the equivalent plate representation. This extension allows modeling of unsymmetric wing cross sections, which can arise from airfoil camber or from having different thicknesses in the upper and lower cover skins. This capability is included in the formulation by adding stretching terms to the deformation of the reference surface, which does not have to be located at the midplane of the wing. The addition of stretching deformations in the reference surface provides fully coupled bending-stretching behavior of a composite plate to be represented.

Presented as Paper 87-0721 at the AIAA/ASME/ASCE/AHS 28th Structures, Structural Dynamics, and Materials Conference, Monterey, CA, April 6–8, 1987; received June 1, 1987; revision received May 9, 1988.

*Senior Research Engineer, Interdisciplinary Research Office, Structures Directorate. Associate Fellow AIAA.

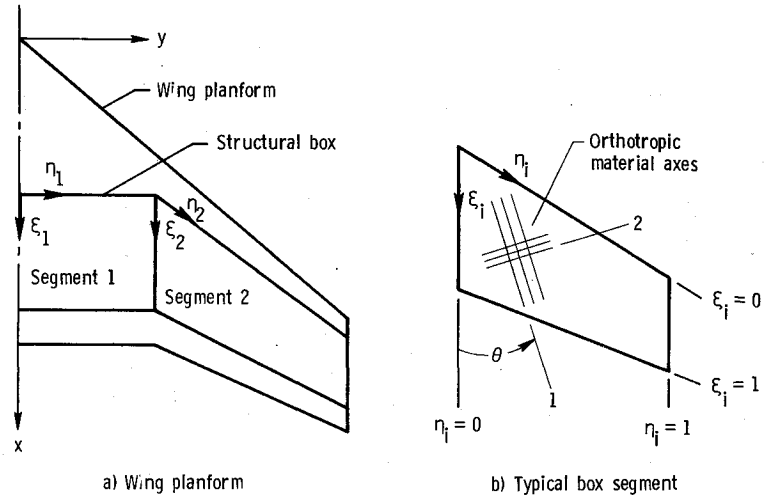

Fig. 1 Coordinate systems used to define wing box structure.

Inplane loads can also be applied in this generalized formulation. An implementation of thermal loadings, which are described as temperature distributions over the planform of the cover skins, has been included. Spring supports have been added to provide for a more general set of boundary conditions.

The paper will include a description of the analytical formulation along with an example to demonstrate the additional features. Results will be presented to assess the effect of wing camber on the static and dynamic response of an example wing structure under pressure and thermal loading. These results will be compared with corresponding results from a finite-element analysis program to indicate how well a cambered wing box can be represented with a flat-plate formulation.

It is assumed that the reader of this paper is familiar with Ref. 5, which contains a description of the basic method. The material contained in this paper will focus on providing a description of extensions to the previous work and will repeat only a minimal amount of information contained in Ref. 5.

Analytical Modeling

The wing box structure is represented as an equivalent plate in this formulation. Planform geometry of this equivalent plate is defined by multiple trapezoidal segments as illustrated by the two-segment box in Fig. 1a. The global Cartesian coordinate system has the x axis in the streamwise direction and the y axis in the spanwise direction. A separate local coordinate system is associated with each segment. These local coordinates are nondimensionalized such that ξ refers to a fraction of the local chord and η refers to a fraction of the span for a given segment, as indicated in Fig. 1b. The subscripts on the ξ and η coordinates, shown in Fig. 1 to refer to a particular segment, are omitted in the remainder of this paper since the development of the analysis method is described for a typical segment. The orthotropic material axes, denoted 1 and 2, are also shown in Fig. 1b for a typical layer in the cover skin.

The cross-sectional view of a typical segment in Fig. 2 illustrates the analytical modeling of the wing box structure. The location of the midcamber surface of the wing is defined as the distance zc from a user-specified reference plane. This distance varies over the planform of each segment and is expressed as a polynomial in the global coordinates x and y.

$$zc(x,y) = z_{00} + z_{10}x + z_{20}x^2 + z_{01}y + \cdots + z_{mn}x^m y^n \quad (1)$$

The coefficients z_{mn} are constants that are defined by the analyst for each segment. Similarly, the depth of the structural box, which also varies over the planform, is defined by the analyst again in polynomial form

$$h(x,y) = h_{00} + h_{10}x + h_{20}x^2 + h_{01}y + \cdots + h_{mn}x^m y^n \quad (2)$$

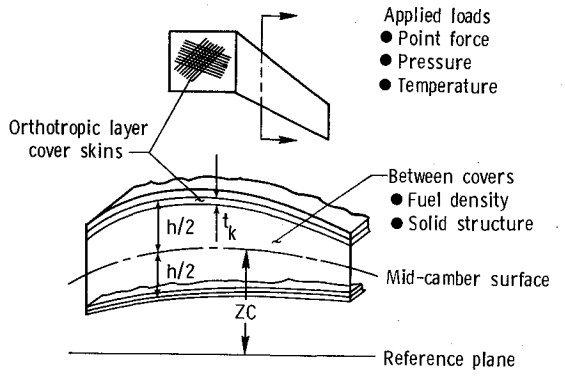

Fig. 2 Analytical modeling of wing box structure.

The cover skins consist of orthotropic layers with the thickness of each layer being defined independently also in polynomial form

$$t_k(x,y) = t_{00} + t_{10}x + t_{20}x^2 + t_{01}y + \cdots + t_{mn}x^m y^n \quad (3)$$

The properties of the layers can be defined to represent wing skins that are stiffened panels or composite laminates. Orientation of the stiffness properties and corresponding thickness are specified for each layer, and the orientations and thicknesses can be different in different planform segments. In the present implementation, the thickness of a layer in the lower skin is specified as a factor times the thickness of the corresponding layer in the upper skin. This simplification is implemented to reduce the number of variables that must be considered in a design application of this procedure. The exponents of the polynomial terms m and n are not necessarily the same for Eqs. (1–3). These exponents are specified by the analyst and values of the fourth power have been found sufficient for representing a fairly general class of wing box geometry.

New options have been added for modeling the volume between the covers. This volume can be 1) considered empty to represent a dry wing, 2) used to represent fuel by assigning a fuel density, or 3) specified as solid structure by giving material stiffness properties. Option 3 is provided to analyze wind-tunnel models for conditions where aeroelastic effects may be important. Although not shown in Fig. 2, rib and spar caps can be represented as axial elements, and concentrated masses can be defined for vibration analysis, as described in Ref. 5.

Thermal loading is included for static analysis along with concentrated forces and distributed pressure loads. Thermal loads are specified as temperature distributions over the planform of the cover skins. The temperature is assumed constant

through the thicknesses of all layers making up the skin. In the present procedure, the material properties of the skins are not considered to be a function of temperature.

Energy Expression for Plates

An expression for the strain energy of a plate segment is needed for the Ritz solution procedure that is used. This expression is developed in terms of bending and stretching of the reference plane shown in Fig. 2. The Kirchhoff assumption is made that lines normal to the reference plane remain straight and normal under deformations of the equivalent plate. This condition is analogous to the assumption that cross sections of a beam remain plane and normal to the centroidal axis in beam theory. The deformations in the equivalent plate are given as

$$U = U_0 - zW_{,x} \tag{4a}$$

$$V = V_0 - zW_{,y} \tag{4b}$$

$$W = W \tag{4c}$$

where U_0 and V_0 refer to stretching of the reference surface in the x and y directions at $z = 0$, and W is a deformation normal to the surface caused by bending. Corresponding strains in the x and y directions are given by

$$\varepsilon_x = U_{0,x} + 0 \quad - zW_{,xx} \tag{5a}$$

$$\varepsilon_y = 0 \quad + V_{0,y} - zW_{,yy} \tag{5b}$$

$$\varepsilon_{xy} = U_{0,y} + V_{0,x} - 2zW_{,xy} \tag{5c}$$

In order to include thermal loading, the total strain ε is separated into the sum of stress-induced components ε' and temperature-induced components ε'', as in Ref. 6. These strains can be expressed for each layer in the cover skins in terms of orthotropic material properties along the axes 1 and 2 as

$$\begin{Bmatrix} \varepsilon_1 \\ \varepsilon_2 \\ \varepsilon_{12} \end{Bmatrix} = \begin{bmatrix} S_{11} & S_{12} & 0 \\ S_{12} & S_{22} & 0 \\ 0 & 0 & S_{66} \end{bmatrix} \begin{Bmatrix} \sigma_1 \\ \sigma_2 \\ \sigma_{12} \end{Bmatrix} + \begin{Bmatrix} \alpha_1 \Delta T \\ \alpha_2 \Delta T \\ 0 \end{Bmatrix} \tag{6}$$

where the vector produced by multiplying the matrix and vector following the equal sign in Eq. (6) is ε', and the vector following the summation sign is ε''. The stresses and stress-induced strains in each lamina are transformed to the global (x,y) coordinate system and used in the expression for strain energy as

$$\Pi = 1/2 \int_{\text{vol}} (\sigma_x \varepsilon'_x + \sigma_y \varepsilon'_y + \sigma_{xy} \varepsilon'_{xy})\, dV \tag{7}$$

This energy expression can be written in terms of total strains as the sum of two parts, $\Pi = \Pi_1 + \Pi_2$.

$$\Pi_1 = 1/2 \int_{\text{vol}} \{\varepsilon\}^T [Q^k] \{\varepsilon\}\, dV \tag{8a}$$

$$\Pi_2 = -1/2 \int_{\text{vol}} \{\alpha\}^T [Q^k] \{\varepsilon\}\, dV \tag{8b}$$

where $\{\varepsilon\}^T = \{\varepsilon_x\ \varepsilon_y\ \varepsilon_{xy}\}$ are total strains, $\{\alpha\}^T = \{\alpha_x\ \alpha_y\ \alpha_{xy}\}$ are "effective" thermal coefficients as discussed in Ref. 7, and $[Q^k]$ is a lamina stiffness matrix.

The strain energy of the plate is given by Eq. (8a), and the potential energy of the thermal loading is given by Eq. (8b). When the strain energy of the plate from Eq. (8a) is expanded in terms of the reference surface displacements in Eqs. (5), a total of 28 terms result, as given in Ref. 8. Note that for bending alone there are only 6 terms in the energy expression, as given in Ref. 5. Therefore, the addition of the stretching deformations to handle cambered wing boxes requires considerable additional computation.

Analysis Procedure

The Ritz method is used to obtain an approximately stationary solution to the variational condition on the energy of the structure and applied loads. In this application of the Ritz approach, each component of the deformation of the reference surface is assumed to be the sum of contributions from sets of specified displacement functions

$$U = \sum_i A_i X(x)_i Y(y)_i \tag{9a}$$

$$V = \sum_j B_j X(x)_j Y(y)_j \tag{9b}$$

$$W = \sum_k C_k X(x)_k Y(y)_k \tag{9c}$$

As in Ref. 5, these displacement functions are specified as products of terms from a power series in the x direction with terms from a power series in the y direction. Different sets of functions can be used for the U, V, and W components of the deformation.

For static analysis, the Ritz procedure, as described in Ref. 5, produces a system of simultaneous equations which can be solved for the unknown coefficients in Eqs. (9) to minimize the total energy expression. These equations can be written in partitioned matrix form as

$$\left[\begin{array}{c|c|c} K_{uu} & K_{uv} & K_{uw} \\ \hline K_{vu} & K_{vv} & K_{vw} \\ \hline K_{wu} & K_{wv} & K_{ww} \end{array}\right] \left\{\begin{array}{c} A \\ \hline B \\ \hline C \end{array}\right\} = \left\{\begin{array}{c} P_u \\ \hline P_v \\ \hline P_w \end{array}\right\} \tag{10}$$

These equations represent the fully coupled bending-stretching behavior of a composite plate.

The evaluation of the terms in the submatrices of the stiffness matrix of Eq. (10) requires the integration of the strain energy in Eq. (8a) over the volume of structural material. This integration involves functions of the camber shape zc, the wing depth h, and the thickness of each cover skin layer t_k, along with the corresponding lamina stiffness matrix Q^k. To simplify calculations and make the resulting stiffness matrix a linear function of layer thickness, all layers in a skin are assumed to be located at the same distance from the reference surface.

During integration their thicknesses are simply summed to yield the appropriate stiffness values. This simplification is invalid for plates with a small distance between the covers but results in only a small error for typical wing structures where the depth of the wing is large compared to the thickness of the covers. Exact integral expressions are formed and evaluated at limits on the upper and lower covers for the material between the covers. The expressions describing the model shown in Eqs. (1–3) must be combined with quadratic functions of the strains, hence displacement functions, as given in Eq. (5) to complete the expression for strain energy of the plate as shown in Eq. (8a). The formation and evaluation of the terms in these integral expressions is algebraically cumbersome and involves tedious manipulations. However, the mathematical operations involved yield polynomials in x and y and the same library of subroutines that were developed in Ref. 5 are used to perform all the mathematical operations on these polynomials in an efficient manner.

Thermal Loads

Thermal loading is included for static analysis along with concentrated forces and distributed pressure loads. Thermal loads are specified as temperature distributions over the planform of the cover skins. The temperature is assumed constant through the thicknesses of all layers in the skin. The thermal loads are calculated using Eq. (8b). The thermal coefficients

that are needed for each layer are transformed to the global x-y coordinate system by

$$\alpha_x = \cos^2\theta\alpha_1 + \sin^2\theta\alpha_2 \quad (11a)$$

$$\alpha_y = \sin^2\theta\alpha_1 + \cos^2\theta\alpha_2 \quad (11b)$$

$$\alpha_{xy} = 2\sin\theta\cos\theta(\alpha_1 - \alpha_2) \quad (11c)$$

where θ is the angle from the x axis to the 1 axis of the orthotropic material. At present, the stiffness properties of the layers Q are not considered to be a function of temperature in the analysis procedure.

If the temperature distribution $\Delta T(x,y)$ is input as a polynomial, the necessary integrations are performed using closed-form expressions. Often, the temperatures have been calculated in a separate program on a grid over the wing planform. In this case, numerical integration can be performed with the appropriate values of temperature, thermal and stiffness coefficients, strain, and planform area associated with each point in the grid being used. This integration must be performed for each of the displacement functions that are used in the analysis as described in Ref. 5. This procedure is analogous to the procedure used for application of aerodynamic pressure loads in the equivalent plate formulation.[9,10]

The capability to consider both aerodynamic and thermal loading indicates a potential use of this procedure for static aerothermoelastic calculations for advanced vehicles where aerodynamic heating is an important design consideration. Such calculations would involve an iteration on a combination of thermal loads, structural deformations, and aerodynamic loads to arrive at a set of loads that are consistent with the deflected shape of the loaded wing at some specified flight condition.

Definition of Constraints

For static analysis, rigid-body motion of the plate must be constrained. These constraints are often referred to as boundary conditions. In Ref. 5, the example equivalent plate wing model was clamped along the x axis, which represented an aircraft centerline. This is accomplished by excluding selected terms from the set of displacement functions as follows:

1) The condition that the displacement W is zero at $y = 0$ can be specified by excluding all terms containing y to the zero power y^0 from the set of displacement functions.

2) The condition that the slope $W_{,y}$ is zero at $y = 0$ can be specified by excluding all terms containing y to the first power y^1 from the set of displacement functions.

3) Clamped conditions at $y = 0$ are specified by imposing both 1 and 2.

This method of specifying constraints is limited to the x and y axes. Other methods of applying constraints, which are available in the literature,[11] were evaluated as candidates to provide for specification of more general types of boundary conditions. The Lagrange-multiplier method allows exact specification of constraints but at the expense of introducing additional equations with zeros on the diagonal. The method selected for use is an adaptation of the penalty-function method discussed in Ref. 11. This method will only satisfy the constraints approximately. A penalty number is used, and the larger the penalty number the better the constraints will be achieved. For the purposes of constraining the equivalent plate, this penalty number is taken to be the stiffness of a spring at the location of the desired constraint. Such springs can resist translation or rotation and are defined at a point or distributed along a specified line. Although displacements cannot be specified to be exactly zero at a selected location, use of sufficiently stiff springs will provide a good approximation to the desired condition.

A combination of excluding terms from the displacement functions and application of stiff springs is used to define the constraints on the example wing, which will be discussed in a later section of this paper. The input data used to define the displacement functions for the analysis are given in Table 1. The directions refer to the U,V,W deformations, and NX and NY indicate the number of terms to be used in the x and y directions, respectively. The displacement function in each direction is composed of a polynomial containing the sum of terms from all combinations of the x and y powers that are given. Constraints for the example are imposed by omitting terms containing y^0 from the V deformation to provide a deflection constraint at $y = 0$ and by omitting terms containing y^1 from the W deformation to constrain the slope at $y = 0$.

Table 1 Input data used to define displacement functions

Directions	NX	x powers	NY	y powers
1	5	0 1 2 3 4	6	0 1 2 3 4 5
2	5	0 1 2 3 4	5	1 2 3 4 5
3	5	0 1 2 3 4	6	0 2 3 4 5 6

In addition to the more general capability for specifying constraints, an eigenproblem shift parameter[12] has been included for use in vibration analysis. This shift parameter allows a vibration analysis to be performed on a model with unconstrained (rigid-body) motions.

Implementation of Method

This equivalent plate analysis procedure is being developed for use with mathematical optimization procedures for application in early preliminary design. Therefore, an important facet of the development is the implementation into a computationally efficient computer program. Although a detailed description of the computer program is beyond the scope of this paper, some of the significant approaches used to achieve the desired efficiency are outlined in this section.

Generation of Stiffness Matrix

The terms associated with calculating coefficients of a stiffness matrix for an anisotropic plate segment are algebraically cumbersome and tedious to manipulate. The general procedure for calculating these terms for only the bending deformation W is described in Ref. 5. To include the stretching deformations U and V, the size of the stiffness matrix is increased, as indicated in Eq. (10). The procedure involves evaluation of the integral shown in Eq. (8a). The strains needed for this evaluation can be written as the sum of components from the U, V, and W deformations as shown in Eq. (4). Each submatrix in Eq. (10) is formed by using the appropriate combination of the components in the various directions.

The procedure is implemented by generalizing the corresponding procedures used for K_{ww} in Ref. 5. These calculations can then be performed by looping through this common set of generalized procedures with the origin of each submatrix and the definition of the strain components being changed at the beginning of each loop to correspond to the desired combination of the U, V, and W directions. The strain components are defined in a table containing the direction, the coefficients, and an indicator to specify the proper derivative operation.

Integral Tables

The evaluations outlined above are performed for all combinations of terms that are specified in the displacement functions for each direction in order to complete a submatrix. All these evaluations involve generation and integration of lengthy polynomial expressions. Since these expressions are all sums of terms containing a coefficient multiplied by $x^m y^n$, tables are generated with each entry containing the integral of such terms over the planform of the segment being evaluated for all combinations of m and n that are required. Entries in the table are evaluated by integrating over the unit square for each plate segment after expressing the terms in the local coordinate system. The coordinate transformations are given in terms of the

planform variables shown in Fig. 3 as

$$x = e + a\xi + (f - e)\eta + (c - a)\xi\eta \tag{12}$$

$$y = g + b\eta \tag{13}$$

The coordinate transformation of the differential area is given by the determinant of the Jacobian as

$$dx\, dy = [ab + (c - a)b\eta]\, d\xi\, d\eta \tag{14}$$

The distance from the reference surface to either the upper or lower cover skin is indicated by the symbol z in the expression for the W component of strain in Eqs. (5). This distance can be expressed in polynomial form in terms of the midcamber and wing-depth definitions given in Eqs. (1) and (2). The maximum power of z is 2 for the pure bending K_{ww} submatrix for cover skins and 3 after integrating through the wing depth for solid plates. In the implementation used herein, eight integral tables are generated corresponding to the 0, 1, 2, and 3 powers of z for the upper and lower surfaces. The tables contain evaluations of terms corresponding to $z^j \times x^m y^n$ that are used to generate the stiffness submatrices for appropriate combinations of strain components.

Input of Analytical Model

The definitions of the midcamber surface, wing depth, and thicknesses of layers in the cover skins are given in terms of the global coordinates in Eqs. (1–3). Such a definition results in all subsequent polynomials that are generated being the sum of $x^m y^n$ terms. Retaining this form allows the efficient handling of the integral operations as described above. An input option is provided for defining the model directly in the x-y coordinate system. However, it is often more convenient for the user to input these quantities in the local ξ-η coordinate system of each segment as was done in Ref. 5. This input option has been included in the present implementation but a transformation from the ξ-η system to the global x-y system is necessary. A direct transformation using the inverse of Eqs. (12–14) results in a complicated form rather than the desired simple power series polynomials. Therefore, an approximate transformation to the power series polynomials is used.

This approximate method minimizes the square of the difference between the input polynomial in the ξ-η system and a power series polynomial in the x-y system integrated over the planform of the segment. The function to be minimized can be written as

$$\Omega = \int_{\text{area}} (F - G)^2\, dA$$

$$= 2\int_{\text{area}} (1/2G^2 - FG + 1/2F^2)\, dA \tag{15}$$

where $F = f(\xi,\eta)$ which is input, and $G = g(C_{mn}x^m y^n)$ is the desired polynomial. Differentiating Eq. (15) with respect to the unknown coefficients C_{mn} yields a set of simultaneous equations that can be generated and solved using the same procedures as that for the potential energy given in Eqs. (8). This solution is the desired surface fit and the procedure can be used to obtain the coefficients for Eq. (1–3) to define an analytical model.

Analysis Time

The time required to perform an analysis includes the time required for input preparation to define the analytical model, the execution time of the program, and time required for the analyst to assimilate the output data. The specification of model characteristics as continuous distributions in polynomial form requires only a small fraction of the volume of input data for a corresponding finite-element structural model where geometry and stiffness properties are specified at discrete locations. Equivalent plate models are applicable for cases where the stiffness can be represented as a continuous distribution within segments, therefore limiting the complexity of modeling.

The execution time is a function of complexity and refinement of the analytical model. The number of degrees of freedom used in an analysis to give adequate accuracy is problem dependent. Results are presented in this paper for two different sets of displacement functions for the equivalent plate model and for two different element mesh refinements for the finite-element model. Computational times and selected results are compared to give an indication of the accuracy and computational efficiency of these procedures for different levels of modeling.

The number of degrees of freedom in an equivalent plate model is readily changed by simply changing the specification of terms in the displacement functions rather than refining the number of joints and elements in a finite-element model. The output quantities such as displacements, strains, stresses, and vibration-mode shapes are calculated on a user-specified grid over each plate segment. Since the definitions of these quantities are given as continuous polynomials, the grid can be as fine or as course as desired. Presently, no graphical presentation of output data has been implemented.

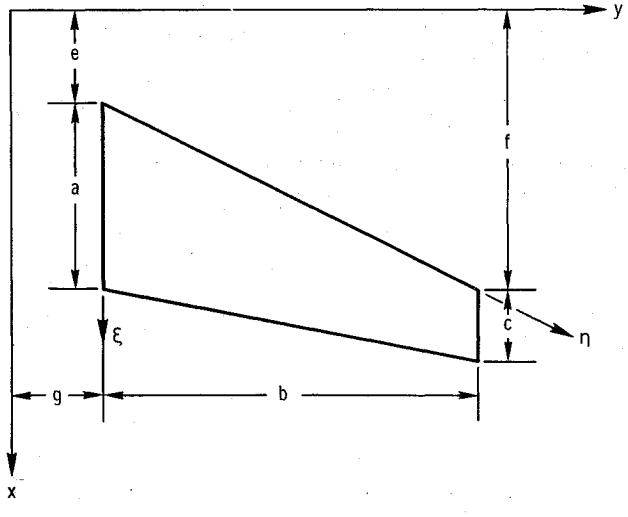

Fig. 3 Planform geometry variables for typical segment.

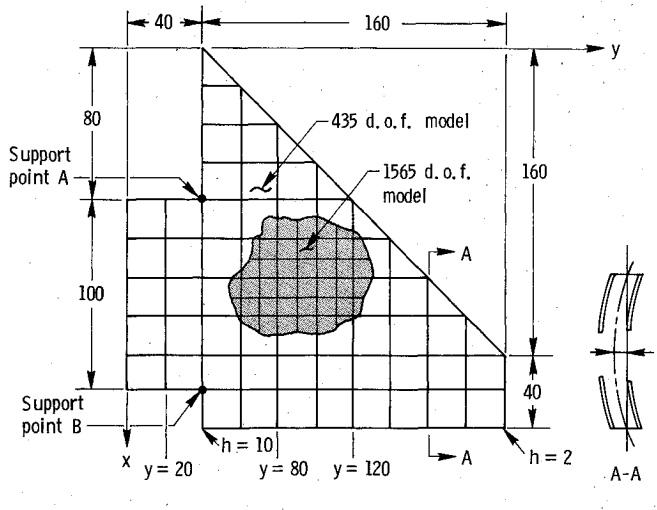

Fig. 4 Planform of example wing box; dimensions in inches.

Application and Results

Model Description

The planform of an example wing box that is being used to evaluate the effects of using camber in the formulation is shown in Fig. 4. A two-segment planform, representative of a fighter aircraft wing, is used for testing purposes. The planform is composed of a clipped-delta outer segment with a 45 deg leading edge sweep and an inner segment to represent a carry-through structure. A delta planform is selected for evaluation because cambering of the long chord length in the inboard portion of the wing leads to significant changes in the z coordinate of the wing surfaces. Two loading conditions were used for testing. The first is an externally applied loading of a uniform 1-psi acting over the planform of the outer segment. The second is a thermal loading that is specified as the temperature of the lower surface of the wing segment being 100°F greater than that of the upper surface. Boundary conditions are imposed by 1) excluding selected terms from the displacement functions as described in an earlier section to constrain the slope of the bending deflection W and the spanwise stretching deflection to zero at $y = 0$, and 2) using stiff springs (spring constants all set equal to 1.0×10^5) at the locations denoted as support point A and support point B in Fig. 4. These springs all have one end fixed, and the translation of the other end is equal to the deflection of the equivalent plate at the points specified. The axis of each spring is oriented in a direction to constrain specified deflections of the plate. At support point A, one spring is oriented in the x direction to constrain the U deflection and another is oriented in the z direction to constrain the W deflection. At support point B, a single spring in the z direction is used to constrain the W deflection.

A simple expression for the shape of the midcamber surface is used to evaluate the effects of camber. This shape is specified as a quadratic function of the chord length (parabolic arc) with the maximum dimension zc_{max} located at 50% chord location. The amount of camber will be defined as Φ, where $\Phi = zc_{max}/$ local chord. Results are presented for no camber (symmetric wing) and a camber of $\Phi = 0.03$. The equivalent plate analysis for the cambered wing is performed using two different sets of displacement functions for the bending deflection W. The first set, referred to as the 4×6 analysis, has the exponents shown earlier in the discussion of constraints, with 4 being the largest exponent in the x direction and 6 being the largest exponent in the y direction. In the second set, which is referred to as the 5×5 analysis, 5 is the largest exponent in both the x and y directions.

Results from the equivalent plate analysis for the cambered wing are compared with corresponding results from the EAL finite-element analysis program.[12] The engineering analysis language (EAL) model is built up of membrane rib, spar, and cover elements with the grid of cover elements shown in Fig. 4. Analyses are performed for two levels of modeling. One model has a grid of cover elements with twice the refinement as the other model in both the x and y directions and has additional rib and spar elements corresponding to the edges of each cover element. The models will be referred to as the 435 degree-of-freedom (DOF) model and the 1565 DOF model, as indicated in Fig. 4.

Numerical Results

The relative level of accuracy of results and corresponding computational time for the different models used to analyze the cambered wing box structure are presented in Table 2. A measure of the overall accuracy is given by the total strain energy of the deformed structure for the pressure and thermal load cases. Increased accuracy is indicated by an increasing value of strain energy, so that the 1565 DOF finite-element model is shown to provide the best overall results in this study. The corresponding increase in computational time required to provide the improved accuracy is also shown in Table 2. The equivalent plate analyses required less computational time than the finite-element analyses. However, the magnitude of the difference is very dependent on the level of modeling used. Values of deflections and stresses at selected locations on the wing along with vibration frequencies are presented in the remainder of this section to provide a detailed comparison of results.

Static displacements for the uniform pressure load are presented along the trailing edge of the wing in Fig. 5. These results indicate that camber reduces the deflection by approximately 5% at the wing tip. This relatively small difference suggests that a flat representation of a cambered wing may be adequate for aeroelastic calculations. The difference between the deflections from the 4×6 and the 5×5 equivalent plate models are negligible so that only results from the 4×6 model are shown in Fig. 5. The deflection obtained from the finite-element model of the cambered wing with 435 DOF is in close agreement with that obtained from the equivalent plate

Table 2 Comparison of strain energy and computational time for different levels of structural modeling

Model	Strain energy, in.-lb: Pressure load	Strain energy, in.-lb: Thermal load	Computation time, s
Eq. plate 4×6	19660.7	78874.0	50.9
Eq. plate 5×5	19700.1	78917.6	54.7
FEM 435 DOF	19919.9	81211.5	122.0
FEM 1565 DOF	21216.6	81897.9	588.0

Table 3 Comparison of natural frequencies from vibration analysis

No.	Eq. plate, $\Phi = 0$: 4×6 model	Eq. plate, $\Phi = 0.03$: 4×6 model	Eq. plate, $\Phi = 0.03$: 5×5 model	FEM, $\Phi = 0.03$: 435 DOF	FEM, $\Phi = 0.03$: 1565 DOF
1	16.24	16.52	16.52	16.38	15.90
2	53.46	54.54	54.41	51.89	52.58
3	80.63	77.23	77.17	72.27	72.56
4	83.01	82.01	82.06	79.63	81.08
5	88.65	93.72	93.12	80.58	82.20
6	127.54	128.28	128.83	119.43	124.28
7	184.06	185.06	180.68	173.09	173.30
8	192.34	193.81	191.36	178.77	185.71
9	212.40	213.60	207.06	199.33	199.57
10	227.48	231.32	233.87	218.25	214.80

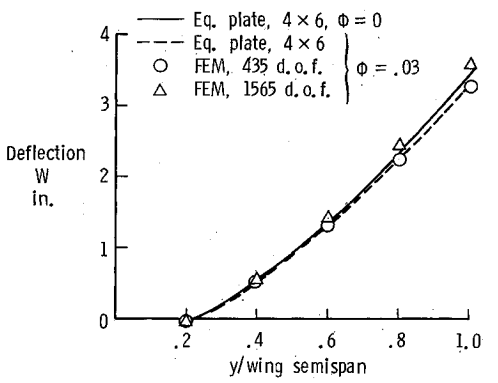

Fig. 5 Deflection of trailing edge of wing box.

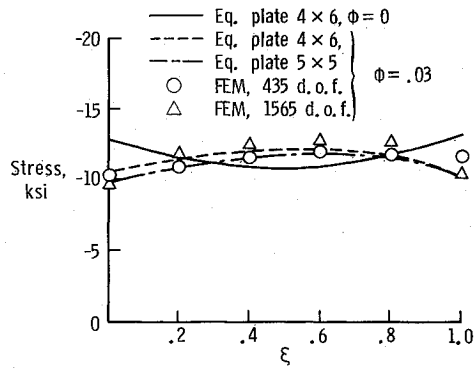

Fig. 6a Stress distribution at $y = 20$, top cover.

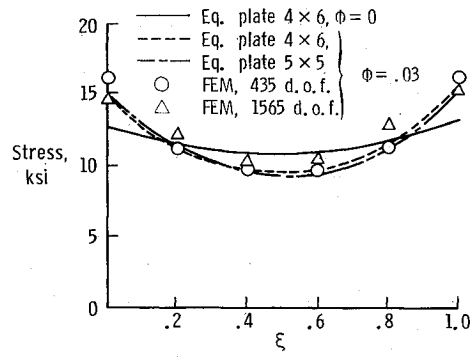

Fig. 6b Stress distribution at $y = 20$, bottom cover.

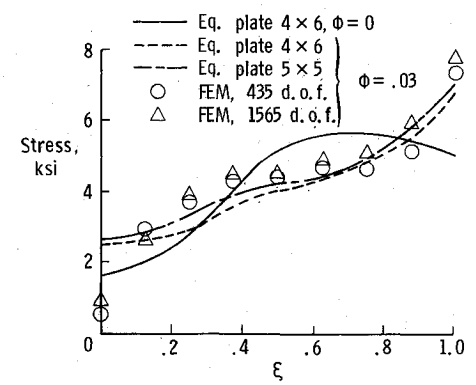

Fig. 7a Stress distribution at $y = 80$, top cover.

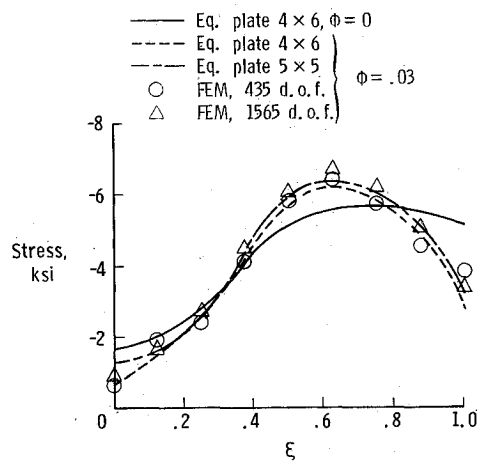

Fig. 7b Stress distribution at $y = 80$, bottom cover.

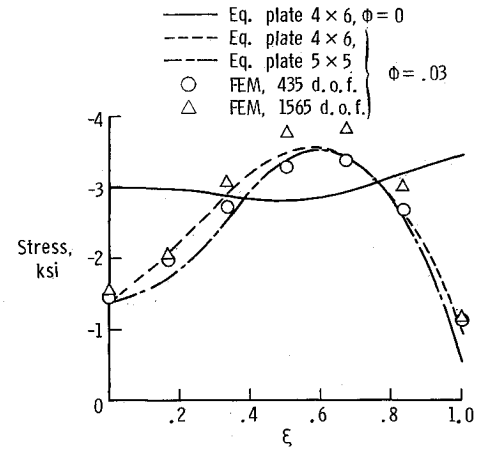

Fig. 8a Stress distribution at $y = 120$, top cover.

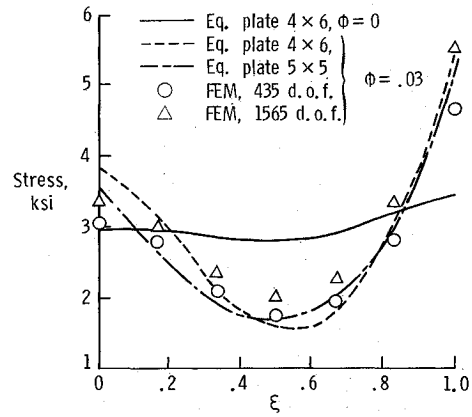

Fig. 8b Stress distribution at $y = 120$, bottom cover.

method. However, these deflections are lower than those given by the 1565 DOF finite-element model.

Distributions of the stress in the spanwise direction for the upper surface and lower surface of the wing are shown in Figs. 6–8. These distributions are given at the $y = 20$, 80, and 120 locations shown in Fig. 4. In some regions there are significant differences between the stresses for a flat wing and the stresses for a cambered wing. For example, this difference is as large as a factor of 2 at some points of the $y = 120$ location. These results indicate the importance of considering camber if the analysis is used in a procedure to size cover skins for strength requirements since the resized thicknesses are proportional to the calculated stresses.

In general, the agreement in stresses for the equivalent plate procedure and the finite-element analysis is acceptable for use during preliminary design. The largest difference occurs in the bottom surface at the $y = 80$ location. This is the region of transition from the carry-through structure to the outer delta portion and it appears that the degree of the polynomials used for the displacement functions is not large enough to represent the gradients occurring in this region. The 5×5 equivalent plate model gives better agreement than the 4×6 model in this region. Attempts to use larger exponents for this particular problem gave ill-conditioned equations that caused the solution subroutine to abort with an error message.

The deflections along the leading and trailing edges of the wing box produced by a temperature differential of 100°F on the lower surface of the wing are shown in Fig. 9. A negative 0.6 deg angle of attack is produced at the wing tip. Such twisting of the wing that occurs from this thermal loading could affect aerodynamics loads and indicates a potential use of this procedure for aerothermoelastic calculations.

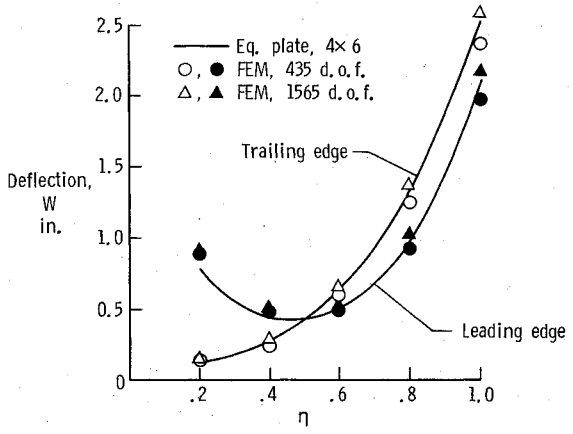

Fig. 9 Thermal deflection of wing box.

Vibration frequencies calculated for the cambered and uncambered wings are shown in Table 3. Camber was found to have only a small effect on the values of the first 10 frequencies. The values of frequencies from the equivalent plate analyses are higher than those from the finite-element analyses, indicating that the displacement functions that were used did not represent the vibrational behavior of the wing as well as the finite-element model. However, the level of accuracy of the frequencies indicate that the equivalent plate method provides an acceptable representation of the vibration characteristics of the wing for use during preliminary design.

Concluding Remarks

A description is given of a further generalization of the equivalent plate formulation to provide capability to model aircraft wing structures with unsymmetric cross sections. The analytical procedures used to provide this capability are given along with some of the methods used for implementing these procedures into a computer program.

Some typical numerical results are presented to assess how well a cambered wing box can be represented by a plate formulation. In general, the difference in results between static displacements and vibration frequencies for the cambered wing example and a flat representation is less than 10%. However, the difference in stresses is significant, as much as a factor of 2 in some regions. This large difference in stresses indicates the importance of including the effects of camber in a general structural resizing procedure.

The degree of the polynomials used for the displacement functions was limited by ill-conditioning of the resulting equations and the same level of accuracy of the finite-element results could not be achieved with the equivalent plate procedure. However, the results from the equivalent plate analyses exhibited the same trends and approached the accuracy of the finite-element analysis results. Considerably less total analysis time was required to generate the equivalent plate results.

In summary, the application of the generalized equivalent plate analysis procedure to cambered wing structures is shown to produce results with adequate levels of accuracy in a shortened analysis time. Hence, the procedure provides a useful capability for the analysis of aircraft structures during early preliminary design.

References

[1]Stroud, W. J., Dexter, C. B., and Stein, M., "Automated Preliminary Design of Simplified Wing Structures to Satisfy Strength and Flutter Requirements," NASA TN D-6539, Dec. 1971.

[2]McCullers, L. A. and Lynch, R. W., "Dynamic Characteristics of Advanced Filamentary Composite Structures," AFFDL-TR-73-111, Vol. II, Sept. 1974.

[3]Lynch, R. W., Rogers, W. A., and Braymen, W. W., "An Integrated Capability for the Preliminary Design of Aeroelastically Tailored Wings," AIAA Paper 76-912, Sept. 1976.

[4]Triplett, W. E., "Aeroelastic Tailoring Studies in Fighter Aircraft Design," AIAA Paper 79-0725, April 1979.

[5]Giles, G. L., "Equivalent Plate Analysis of Aircraft Wing Box Structures with General Planform Geometry," *Journal of Aircraft*, Vol. 23, Nov. 1986, pp. 859–864.

[6]Tauchert, T. R., *Energy Principles in Structural Mechanics*, McGraw-Hill, New York, 1974, Chap. 8, pp. 170–172.

[7]Jones, R. M., *Mechanics of Composite Materials*. Scripta, Washington, DC, 1975, Chap. 4, pp. 193–198.

[8]Ashton, J. E. and Whitney, J. M., *Theory of Laminated Plates*. Progress in Materials Science Series, Vol IV, Technomic Publishing, 1970, Stamford, CT, Chap. 3, pp. 31–33.

[9]Pittman, J. L. and Giles, G. L., "Combined, Nonlinear Aerodynamics, and Structural Method for the Aeroelastic Design of a Three-Dimensional Wing in Supersonic Flow," AIAA Paper 86-1769, June 1986.

[10]Tatum, K. E. and Giles, G. L., "Integrating Nonlinear Aerodynamic and Structural Analysis for a Complete Fighter Configuration," AIAA Paper 87-2863, Sept. 1987.

[11]Zienkiewicz, O. C., *The Finite Element Method*, 3 ed. McGraw-Hill, United Kingdom, 1977, Chap. 3, pp. 77–89.

[12]Whetstone, W. D., "EISI-EAL Engineering Analysis Language Reference Manual—EISI-EAL System Level 2091," Engineering Information Systems Inc., San Jose, CA, July 1983.